IEEE Access
Multidisciplinary | Rapid Review | Open Access Journal

Received September 26, 2019, accepted October 20, 2019, date of publication October 23, 2019,
date of current version September 16, 2020.

*Digital Object Identifier 10.1109/ACCESS.2019.2949120*

# A Multiposition Initial Alignment Method of Portable MIMU/FOG Compound Navigation System

**XIAOWEN CAI, CHUNXI ZHANG, YANQIANG YANG, SHUANG GAO, AND RUOYU ZHANG**
Institute of Optics and Electronics, School of Instrumentation and Optoelectronics Engineering, Beihang University, Beijing 100191, China
Corresponding author: Yanqiang Yang (18811799659@163.com)

**ABSTRACT** In the future, a pedestrian navigation system (PNS) will be widely applied. In navigation system, an initial alignment is essential before starting navigation. There are two primary alignment methods, one is an inertial/magnetometer assisted alignment method, the other is a multiposition rotation modulation alignment method. However, magnetometer is susceptible to magnetic disturbance, and the large volume of rotary modulation system is not suitable for PNS. To solve these problems, a compound navigation system (CPNS) is proposed. It consists of a single-axis fiber-optic gyro (FOG) and a triaxial microelectromechanical system inertial measurement unit (MIMU) without modulation mechanism. CPNS is placed in different positions. According to the variation law of cosine function, FOG data in multiposition are used as fitting alignment, MEMS gyro tracks attitude changes between different positions. The experimental results demonstrate that initial alignment accuracy can be well calculated with several multiposition schemes under different conditions. This method could be a novel solution for PNS's initial alignment.

**INDEX TERMS** Least squares method, MIMU/FOG compound navigation system, multiposition, initial alignment.

## I. INTRODUCTION

Because there is a need to develop weapons that do not rely on a satellite navigation system [1], the Defense Advanced Research Projects Agency launched the Micro-Technology for Positioning, Navigation and Timing program in 2010 [2], [3]. PNS is the key research direction in the program. In navigation systems, it is essential to determine the initial values of attitude angles (i.e., initial alignment) before starting navigation. High accuracy IMUs can perform initial alignment without other sensors in a less disturbed environment, but their weight and cost limit their use in PNS. Over last decades, the performance and accuracy level of MIMU have been continuously improved. Due to its outstanding advantages [4], [5], MIMU has become a research focus in the navigation field. For MIMU, the initial alignment cannot be directly achieved because microelectromechanical system (MEMS) sensors have high noise and instability characteristics [6], [7]. Many studies have been carried out to improve the MIMU performance to accomplish the initial alignment of the MIMU [8]–[10]. Two primary methods can be applied to improve the performance of MIMU. One is an inertial/magnetometer assisted alignment method [11]. The other is a multiposition rotation modulation alignment method, in which a turntable is applied to modulate the rotary IMU.

In the inertial/magnetometer assisted alignment method, the attitude information is obtained by a tri-axial magnetometer that can measure a geomagnetic field. Online calibration or periodic calibration is needed before using low accuracy magnetometers. Thus, an integrated compensation model based on the least squares ellipsoid fitting is proposed to compensate the integrated error of the magnetometer [12], [13]. After calibrating the magnetometer, a nonlinear filtering data fusion method is discussed to perform stationary base alignment in [14]–[16]. However, the deterioration of magnetometer accuracy under dynamic attitude tracking, the method is not suitable for the dynamic alignment. To solve the problem, Ludwig [17] used a genetic algorithm to find the optimal weight between the relative orientation from a gyro and the absolute orientation from an accelerometer/magnetometer. The advantage of the

The associate editor coordinating the review of this manuscript and approving it for publication was Ehsan Asadi.

inertial/magnetometer assisted alignment method is short initial alignment time. However, the magnetometer accuracy is easily prone to disturbances from electrical and metal surroundings, and the initial alignment accuracy is low.

To improve the alignment accuracy, a multiposition rotation modulation alignment method, which uses an error compensation technique (i.e., rotating modulation technique), is proposed [18]–[20]. The rotating modulation technique can operate in two modes: multiposition rotating modulation and continuous rotation modulation. In [21]–[24], a multiposition rotation path was designed to reduce the alignment error that is caused by inertial sensor errors. The way to improve alignment accuracy is to increase the number of positions, but the alignment time increases at the same time. To reduce the alignment time, Collin [25] proposed a continuous rotation modulation method, and discussed the effect of rotating modulation on the stochastic error processes of a MEMS gyro. Several real-time continuous rotation modulation methods based on a gyro have been proposed in [26]–[28]. In this method, the inertial sensors error is suppressed by the modulation mechanism. Thus, the long-term alignment accuracy is considerably improved. However, the rotating modulation technique scheme inevitably increases the operation complexity, power supply, and the cost of the navigation system. The large volume of the system is not suitable for PNS.

The characteristics of various primary initial alignment methods are illustrated in Table 1.

**TABLE 1. Characteristics of various traditional methods.**

| | Methods | Applicable scenario | Disadvantages |
|---|---|---|---|
| Magnetometer/IMU integrated method | Ellipsoid fitting | Online calibration or periodic calibration | Low alignment accuracy; Susceptible to interference |
| | Nonlinear filtering data fusion method | Stationary base alignment | |
| | Kalman filter and genetic algorithm | Dynamic attitude tracking | |
| Modulated method | Multiposition rotating modulation | High alignment accuracy system | The modulation mechanism; Large volume; Not suitable for portable use |
| | Continuous rotation modulation | Quick alignment system | |

To overcome the shortcomings of primary methods, this paper presents a simple and rapid initial alignment method. The proposed method aims to achieve the following objectives:

1) A CPNS consisting of a MIMU and a single-axis FOG is proposed to realize the PNS;

2) A MEMS tracking strategy replaces the traditional rotation modulation system and achieves alignment accuracy in the system with small volume and light weight;

3) During the initial alignment process, the MEMS tracking system is isolated from external angular vibrations, which reduces the interference factors such as artificial misoperation.

In this study, the configuration of CPNS is developed. In addition, a multiposition cosine-fitting method aiming to calculate the initial alignment accuracy is introduced. During the process, the least squares method is applied to the cosine-fitting method. Finally, the experimental results demonstrate that the initial alignment accuracy can be calculated with the several multiposition schemes under different conditions.

## II. CONFIGRATION OF CPNS

CPNS is composed of a MIMU and a single-axis FOG, as shown in Fig. 1.

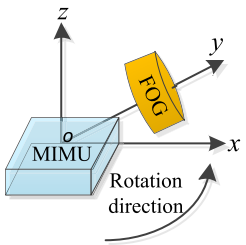


**FIGURE 1. Configuration of CPNS.**

It is assumed that the MIMU body frame coincides with the east-north-up (ENU) frame, and the single-axis FOG is placed along the $y$-axis of the MIMU body frame. CPNS rotates along the $z$-axis. Because FOG is placed on the $o$-$xy$ plane in the body frame, the FOG output $\omega_F$ is the projection of Earth's rotation rate in the navigation frame, which can be described as [29]

$$\omega_F = \omega_{ie}^n \cos\theta \tag{1}$$

where $\omega_{ie}^n$ is the north component of Earth's rotation rate in the navigation frame, and $\theta$ is the intersection angle between the actual position of FOG and the true north direction. Clearly, the FOG output is the cosine modulation of the Earth's rotation rate projection in the rotation plane.

There are two preconditions for the proposed initial alignment method used in CPNS: 1) the system has to be calibrated before the initial alignment; the calibration method and path design are described in [30]. After the installation error compensation, the outputs of FOG and MIMU are unified into the same coordinate system; 2) the FOG accuracy is much higher than that of the MEMS gyro accuracy; thus, the random error of FOG is not considered in (1).

## III. MULTI-POSITION COSINE-FITTING METHOD

### A. PROBLEM FOMULATION

The multiposition method uses only the static location positions. Consider that the output value has the form of a cosine signal with a relative phase difference

$$y(i) = p\cos(qx(i) + \Delta\varphi) + \varepsilon(i) \tag{2}$$

where $y(i)$ is the output value; $i$ is the position index; $p$ is the amplitudes of the signal; $q$ is the angular frequency given by $q = 2\pi\frac{f}{f_s}$, where $f$ is the frequency of the signal and $f_s$ is the sampling frequency; $x(i)$ is the input value; $\varepsilon(i)$ is the residual error. $\Delta\varphi$ is the phase difference between $y(i)$ and $x(i)$.

### B. LEAST SQUARES METHOD

Equation (2) is identical to the general quadratic form of the cosine function written as

$$Z(x, y) = p\cos(qx + \Delta\varphi) - y = \varepsilon \tag{3}$$

To minimize the residual error, the minimum value for the objective function is calculated as

$$\mathbb{Z} = \min \|Z(x_i, y_i)\|^2 \tag{4}$$

where $x_i$, and $y_i$ are the $i$ th position sample.

For $i = 1, 2, \cdots, N$, the matrix form in (3) is expressed as

$$\begin{bmatrix} \cos(q_1x_1 + \Delta\varphi) \\ \cos(q_2x_2 + \Delta\varphi) \\ \vdots \\ \cos(q_Nx_N + \Delta\varphi) \end{bmatrix} \begin{bmatrix} p_1 \\ p_2 \\ \vdots \\ p_N \end{bmatrix} - \begin{bmatrix} y_1 \\ y_2 \\ \vdots \\ y_N \end{bmatrix} = \varepsilon \tag{5}$$

The parameter vector is estimated by minimizing the error

$$A = \begin{bmatrix} \cos(q_1x_1 + \Delta\varphi) \\ \cos(q_2x_2 + \Delta\varphi) \\ \vdots \\ \cos(q_Nx_N + \Delta\varphi) \end{bmatrix}, \quad P = \begin{bmatrix} p_1 \\ p_2 \\ \vdots \\ p_N \end{bmatrix}, \quad B = \begin{bmatrix} y_1 \\ y_2 \\ \vdots \\ y_N \end{bmatrix}$$

The parameter vector is estimated as

$$\mathbb{Z}(P) = (AP - B)^T(AP - B) \tag{6}$$

The minimization problem is solved by the least squares method [31]

$$P^* = \left(A^TA\right)^{-1}A^TB \tag{7}$$

### C. COSINE-FITTING METHOD

#### 1) PITCH ANGLE AND ROLL ANGLE CALCULATION

A transformation from the navigation frame to the body frame can be carried out as three successive rotations about different axes.

Rotate angle $\varphi$ about the navigation frame $z$-axis;

Rotate angle $\theta$ about the new frame $y$-axis;

Rotate angle $\gamma$ about the new frame $x$-axis;

where $\varphi$, $\theta$, and $\gamma$ denote the heading angle, pitch angle, and roll angle, respectively.

MEMS triaxial accelerometers in MIMU are installed along the three axes of the body frame. The projection components of the accelerometer output in the body frame are measured as

$$f^b = \begin{bmatrix} f_x^b & f_y^b & f_z^b \end{bmatrix}^T \tag{8}$$

The accelerometer output in the navigation frame is

$$f^n = \begin{bmatrix} 0 & 0 & g \end{bmatrix}^T \tag{9}$$

The attitude matrix $C_n^b$ from the navigation frame to the body frame can be described as

$$C_n^b = \begin{bmatrix} A_{11} & A_{12} & A_{13} \end{bmatrix} \tag{10}$$

where

$$A_{11} = \begin{bmatrix} \cos\gamma\cos\varphi - \sin\gamma\sin\theta\sin\varphi \\ -\cos\theta\sin\varphi \\ \sin\gamma\cos\varphi + \cos\gamma\sin\theta\sin\varphi \end{bmatrix},$$

$$A_{12} = \begin{bmatrix} \cos\gamma\sin\varphi + \sin\gamma\sin\theta\cos\varphi \\ \cos\theta\cos\varphi \\ \sin\gamma\sin\varphi - \cos\gamma\sin\theta\cos\varphi \end{bmatrix},$$

$$A_{13} = \begin{bmatrix} -\sin\gamma\cos\theta \\ \sin\theta \\ \cos\gamma\cos\theta \end{bmatrix}.$$

$f^b$ can be obtained by the attitude matrix

$$\begin{bmatrix} f_x^b \\ f_y^b \\ f_z^b \end{bmatrix} = C_n^bf^n = \begin{bmatrix} A_{11} & A_{12} & A_{13} \end{bmatrix} \begin{bmatrix} 0 \\ 0 \\ g \end{bmatrix} \tag{11}$$

According to (10) and (11), (12) - (14) can be derived.

$$f_x^b = -g\sin\gamma\cos\theta \tag{12}$$

$$f_y^b = g\sin\theta \tag{13}$$

$$f_z^b = g\cos\gamma\cos\theta \tag{14}$$

The pitch angle and roll angle are [32]

$$\theta = \arcsin\left(\frac{f_y^b}{g}\right) \tag{15}$$

$$\gamma = arctg\left(-\frac{f_x^b}{f_z^b}\right) \tag{16}$$

#### 2) O-XY PLANE IN THE BODY FRAME COMPONENTS OF THE EARTH'S ROTATION RATE

Earth's rotation rate in the body frame can be expressed as

$$\omega_{ie}^b = C_n^b\omega_{ie}^n \tag{17}$$

where $\omega_{ie}^b$ is the Earth's rotation rate in the body frame, $\omega_{ie}^b = \begin{bmatrix} \omega_{iex}^b & \omega_{iey}^b & \omega_{iez}^b \end{bmatrix}^T$; $\omega_{ie}^n$ is the Earth's rotation rate in the navigation frame, $L$ is the local latitude, $\omega_{ie}^n = \begin{bmatrix} 0 & \omega_{ie}\cos L & \omega_{ie}\sin L \end{bmatrix}^T$, and $\omega_{ie}$ is the Earth's rotation rate.

According to (11) and (15), the projection modulus of the Earth's rotation rate in the $o$-$xy$ plane in the body frame is

$$\alpha = \sqrt{\left(\omega_{iex}^b\right)^2 + \left(\omega_{iey}^b\right)^2} = \omega_{ie}\cos L\sqrt{\sin^2\gamma\cos^2\theta + \sin^2\theta} \tag{18}$$

#### 3) COSINE-FITTING METHOD

The relationship between the FOG output and MIMU heading angle can be described as

$$\omega_F(i) = a\cos(b\varphi_M(i) + \Delta\varphi) + \varepsilon \tag{19}$$

where $\omega_F$ $(i)$ is the FOG output; $a$ is the projection modulus of the Earth's rotation rate in the $o$-$xy$ plane in the body frame, which is calculated by (16); $b$ is a constant value for unit conversion; $\varphi_M$ $(i)$ is the track angle in different positions, it is obtained by MIMU attitude updating; $i$ is the position index; $\Delta\varphi$ is the initial heading angle. $\varepsilon$ is the residual error.

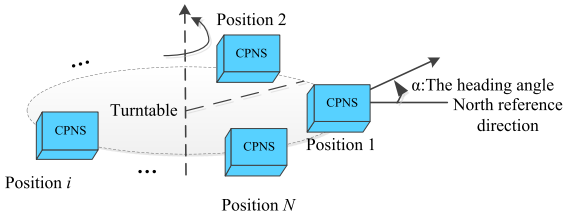


**FIGURE 2.** Different positions of CPNS.

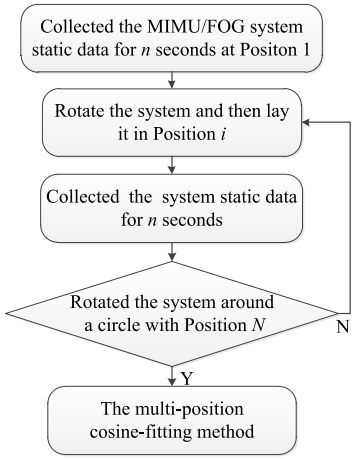


**FIGURE 3.** Initial alignment schematic.

### D. INITIAL ALIGNMENT SCHEME

As shown in Fig. 2, CPNS is placed at different locations in the $o$-$xy$ plane in the body frame. We propose an effective and simple method for the initial alignment, as shown in Fig. 3. The initial alignment scheme is described as follows:

1) Maintain a static state of the initial position, using a MEMS accelerometer to perform the alignment in the $o$-$xy$ plane in the body frame. The pitch angle and roll angle are calculated by (15) and (16);

2) After the alignment, the projection modulus of the Earth's rotation rate in the $o$-$xy$ plane in the body frame is calculated by (18);

3) CPNS is rotated around the $z$-axis in the body frame, and a multiposition static measurement is carried out. During the rotating process, the relative angle between multiposition is obtained by MEMS gyro attitude updating;

4) After the multiposition measurement, the absolute heading angle (angle to the north) $\Delta\varphi$ of the initial position is calculated by fitting the alignment.

## IV. EXPERIMENTAL PROCEDURE AND DISCUSSION

### A. INITIAL ALIGNMENT SCHEME

The hardware design of CPNS is shown in Fig. 4.


**FIGURE 4.** Hardware design of CPNS.

The MIMU uses ADIS16445 [33] which is produced by Analog Devices, Inc., and the single-axis FOG uses a home-built device. The typical performance parameters for CPNS are shown in Table 2.

**TABLE 2.** Typical performance parameters for CPNS.

| Parameters | Typical values | | |
|---|---|---|---|
| | MEMS gyro | MEMS accelerometer | FOG |
| Dynamic range | ±250 °/s | ±5g | ±500 °/s |
| Constant bias | 12 °/h | 0.075mg | 0.02 °/h |
| Angular Random Walk | 0.56 °/ √h | —— | 0.05 °/ √h |
| Velocity Random Walk | —— | 0.073mg/sec/ √hr | —— |
| Noise Density | 0.011 °/s/ √Hz (RMS) | 0.105mg/ √Hz (RMS) | —— |

Numerical experiments are developed. Each sensor output is sampled at a rate of 100 Hz. The system is placed in any initial position and static data is collected for 1 minute. Then, the system is rotated to the next arbitrary position for one circle, and data is collected for 1 minute in each position, for a total of $N$ positions altogether. Of note, each quadrant requires $N/4$ positions to ensure that each of them has an output data of the corresponding position.

The definition of the experiment under different condition is shown in Table 3:

**TABLE 3.** Definition of experiment conditions.

| | Arbitrary positions in east-west-north-south directions | More east-west directions and less north-south directions | All in the east-west directions |
|---|---|---|---|
| Sixteen-position | Case 1 | Case 2 | Case 3 |
| Twelve-position | Case 4 | Case 5 | Case 6 |
| Eight-position | Case 7 | Case 8 | Case 9 |
| Four-position | Case 10 | Case 11 | Case 12 |

To evaluate the CPNS alignment performance, six groups of experiments are conducted in each case.

**TABLE 4. Design of Multiposition CPNS (The black dots represent CPNS positions).**

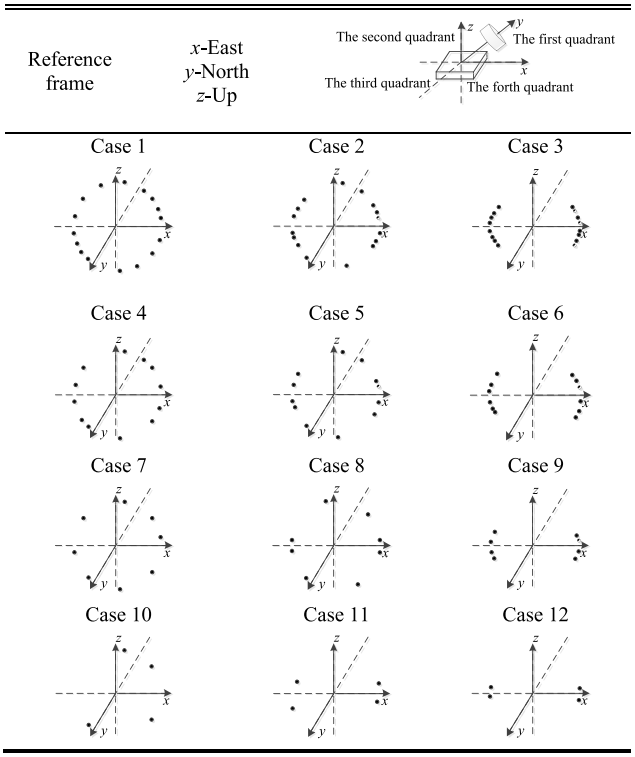


**TABLE 5. Initial alignment accuracy of case 1, case 2, and case 3 (Unit: °).**

| | Case 1 | Case 2 | Case 3 |
|---|---|---|---|
| Group1 | -81.7062 | -83.2532 | -82.8521 |
| Group2 | -81.7635 | -82.3365 | -83.2532 |
| Group3 | -81.1905 | -82.2792 | -82.7375 |
| Group4 | -82.3938 | -82.5084 | -83.3678 |
| Group5 | -81.5916 | -82.4511 | -83.1959 |
| Group6 | -82.9094 | -82.3938 | -83.3678 |
| Mean value | -81.9258 | -82.537 | -83.1291 |
| RMS | 0.6186 | 0.3601 | 0.2698 |

The initial alignment accuracies in sixteen-position are shown in Table 5.

Where RMS is the root mean squared error.

The sixteen-position cosine-fitting results are shown in Fig. 5.

Where (a-1)-(a-6) are Group1-Group6 of Case 1 results, (b-1)-(b-6) are Group1-Group6 of Case 2 results, (c-1)-(c-6) are Group1-Group6 of Case 3 results.

In Fig. 5, the $x$-axis represents the MIMU calculation angle, the $y$-axis represents the FOG output, and the red line is the result of the multiposition cosine-fitting method. Blue dots are distributed arbitrary in each quadrant in Case 1.

Twelve-position, eight-position, and four-position Initial alignment accuracies are shown in Table 6.

The initial alignment accuracy for different cases is summarized in Table 7.

As shown in Table 7, the initial alignment accuracy is improved when the position increases. For the positions with arbitrary angles, the sixteen-position initial alignment

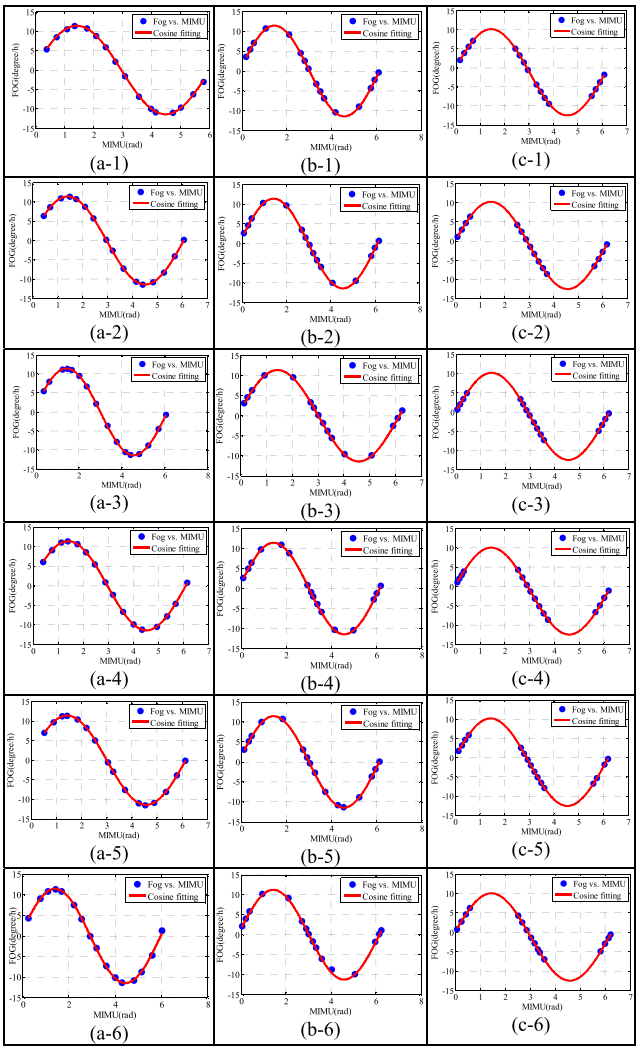


**FIGURE 5. Sixteen-position results.**

accuracy is improved by 59.2% compared with the four-position initial alignment accuracy. In more east-west directions and less north-south directions, the sixteen-position initial alignment accuracy is improved by 31.2% compared with the four-position initial alignment accuracy. In the east-west directions, the sixteen-position initial alignment accuracy is improved by 39.8% compared with the four-position initial alignment accuracy. The experimental results show that for same position number, the more east-west directions have higher initial alignment accuracy. The initial alignment accuracy will be improved with an increase in east-west directions. Similarly, the initial alignment accuracy will improve with the number of positions.

To verify the effectiveness of the proposed method, the initial alignment accuracy of three methods is compared. Method 1 is the auxiliary alignment method of the magnetometer. The total RMS noise of the magnetometer is 0.5mG [34]. Method 2 is the rotation modulation alignment method with motor in the hardware, and the gyro accuracy is 0.2°/h ($1\sigma$) [35]. Method 3 is the proposed method without

**TABLE 6.** Initial alignment accuracy from case 4 to case 12 (Unit: °).

| | Case 4 | Case 5 | Case 6 |
|---|---|---|---|
| Group1 | -83.4251 | -83.4251 | -83.0813 |
| Group2 | -81.7062 | -82.3938 | -83.4824 |
| Group3 | -81.8208 | -82.2219 | -82.9667 |
| Group4 | -81.4197 | -82.6802 | -83.8835 |
| Group5 | -82.5084 | -82.4511 | -83.4251 |
| Group6 | -80.5029 | -81.9927 | -83.5397 |
| Mean value | -81.8972 | -82.5275 | -83.3965 |
| RMS | 0.9922 | 0.4964 | 0.3316 |
| | Case 7 | Case 8 | Case 9 |
| Group1 | -84.5711 | -83.5397 | -83.4251 |
| Group2 | -81.8208 | -82.5084 | -83.5397 |
| Group3 | -81.3624 | -82.2219 | -83.0813 |
| Group4 | -82.4511 | -82.8521 | -84.17 |
| Group5 | -81.8208 | -82.623 | -84.1127 |
| Group6 | -81.9354 | -82.1646 | -83.597 |
| Mean value | -82.3269 | -82.6516 | -83.6543 |
| RMS | 1.153 | 0.5044 | 0.4179 |
| | Case 10 | Case 11 | Case 12 |
| Group1 | -84.2273 | -83.3105 | -83.7116 |
| Group2 | -81.4197 | -81.9927 | -82.8521 |
| Group3 | -81.477 | -82.1646 | -83.9408 |
| Group4 | -80.1019 | -81.9927 | -83.3678 |
| Group5 | -81.5343 | -82.05 | -82.6802 |
| Group6 | -80.0446 | -81.9927 | -83.4824 |
| Mean value | -81.4675 | -82.2505 | -83.3392 |
| RMS | 1.5174 | 0.5236 | 0.4485 |

**TABLE 7.** Initial alignment accuracy for different cases (Unit: °).

| | Arbitrary positions in east-west-north-south directions | More east-west directions and less north-south directions | All in the east-west directions |
|---|---|---|---|
| Sixteen-position | 0.6186 | 0.3601 | 0.2698 |
| Twelve-position | 0.9922 | 0.4964 | 0.3316 |
| Eight-position | 1.153 | 0.5044 | 0.4179 |
| Four-position | 1.5174 | 0.5236 | 0.4485 |

**TABLE 8.** The comparison results between the three methods.

| | Method 1 | Method 2 | Method 3 |
|---|---|---|---|
| RMS | 0.5° | 1° | 0.2698° |

a motor. Using Case 3 of the proposed method as an example, the comparison results are shown in Table 8.

In Table 8, the initial alignment accuracy is improved by 46% compared with the achieved by the magnetometer methods and improved by 73% compared with the rotation modulation alignment method. The result proves the validity of the proposed method.

### B. DISCUSSION

In this section, a series of experiments are performed to validate the feasibility and effectiveness of the proposed method based on CPNS, and the experimental results are discussed in detail. The results prove the superior performance of the proposed method, which successfully improves the initial alignment accuracy. The main advantages of the proposed method are listed below.

1) CPNS has a simple configuration, small size and light weight;

2) The proposed multiposition cosine-fitting method is effective and simple for PNS;

3) Experiments under different conditions are employed to verify the theoretical deduction. Therefore, the requirements for the position can be reduced.

## V. CONCLUSION

The initial alignment is an essential procedure to achieve high-accuracy initial attitude determination for PNS. Aiming to achieve an effective method for the initial alignment, this paper presents two important issues: the configuration of CPNS and the multiposition fitting method. By combining the small size of MIMU and the high accuracy of FOG, a compound configuration of MIMU/FOG is proposed. To fit the FOG output and MIMU attitude information in the approximate *o-xy* plane, a multiposition cosine-fitting method based on the least squares method is proposed to realize the initial alignment. Experiments under different conditions verify the feasibility and effectiveness of the proposed method.

## REFERENCES


[1] G. To and M. R. Mahfouz, "Quaternionic attitude estimation for robotic and human motion tracking using sequential Monte Carlo methods with von Mises-Fisher and nonuniform densities simulations," *IEEE Trans. Biomed. Eng.*, vol. 60, no. 11, pp. 3046–3059, Nov. 2013.

[2] R. Lutwak, "Micro-technology for positioning, navigation, and timing towards PNT everywhere and always," in *Proc. Int. Symp. Inertial Sensors Syst. (ISISS)*, Feb. 2014, pp. 1–4.

[3] A. M. Shkel, "Precision navigation and timing enabled by microtechnology: Are we there yet?" *Proc. SPIE*, vol. 8031, no. 2, 2011, Art. no. 803118.

[4] C. Villalonga, H. Pomares, I. Rojas, and O. Banos, "MIMU-Wear: Ontology-based sensor selection for real-world wearable activity recognition," *Neurocomputing*, vol. 250, pp. 76–100, Aug. 2017.

[5] N. Karthik, "Performance analysis of attitude determination algorithms for low cost attitude heading reference systems," Ph.D. dissertation, Grad. Facul. Auburn, Univ., Auburn, Alabama, 2010.

[6] M. Ismail and E. Abdelkawy, "A hybrid error modeling for MEMS IMU in integrated GPS/INS navigation system," *J. Global Positioning Syst.*, vol. 16, no. 1, p. 6, 2018.

[7] L. Yang, Y. Yang, S. Gao, and R. Li, "Study on the low accuracy IMU's initial alignment technique in the pipeline's geographical coordinate measuring system," *Proc. Eng.*, vol. 29, pp. 2644–2648, 2012.

[8] M. Kumar, B. Mukherjee, K. B. M. M. Swamy, and S. Sen, "A novel design for enhancing the sensitivity of a capacitive MEMS device," *J. Microelectromech. Syst.*, vol. 27, no. 4, pp. 656–666, Aug. 2018.

[9] M. I. Evstifeev and D. P. Eliseev, "Improving the design of moving electrode in MEMS RR-type gyro," *Gyroscopy Navigat.*, vol. 8, no. 4, pp. 279–286, 2017.

[10] U. Qureshi and F. Golnaraghi, "An algorithm for the in-field calibration of a MEMS IMU," *IEEE Sensors J.*, vol. 77, no. 22, pp. 7479–7486, Nov. 2017.

[11] E. Nebot and H. Durrant-Whyte, "Initial calibration and alignment of low-cost inertial navigation units for land vehicle applications," *J. Robotic Syst.*, vol. 16, no. 2, pp. 81–92, 1999.

[12] Q. Li, Z. Li, Y. Zhang, H. Fan, and G. Yin, "Integrated compensation and rotation alignment for three-axis magnetic sensors array," *IEEE Trans. Magn.*, vol. 54, no. 10, Oct. 2018, Art. no. 4001011.

[13] H. Pang, M. Pan, C. Wan, J. Chen, X. Zhu, and F. Luo, "Integrated compensation of magnetometer array magnetic distortion field and improvement of magnetic object localization," *IEEE Trans. Geosci. Remote Sens.*, vol. 52, no. 9, pp. 5670–5676, Sep. 2014.
[14] P. Malinák, M. Soták, Z. Kana, R. Baránek, and J. Duník, "Pure-inertial AHRS with adaptive elimination of non-gravitational vehicle acceleration," in *Proc. IEEE/ION Position Location Navigat. Symp. (PLANS)*, Monterey, CA, USA, Apr. 2018, pp. 696–707.
[15] Z. Hu and Y. Su, "Initial alignment of the MEMS inertial measurement system assisted by magnetometers," in *Proc. IEEE YAC*, Wuhan, China, Nov. 2016, pp. 276–280.
[16] J. K. Lee and E. J. Park, "Minimum-order Kalman filter with vector selector for accurate estimation of human body orientation," *IEEE Trans. Robot.*, vol. 25, no. 5, pp. 1196–1201, Oct. 2009.
[17] S. A. Ludwig and A. R. Jiménez, "Optimization of gyroscope and accelerometer/magnetometer portion of basic attitude and heading reference system," in *Proc. IEEE Int. Symp. Inertial Sensors Syst. (INERTIAL)*, Mar. 2018, pp. 1–4.
[18] H. Xing, Z. Chen, H. Yang, C. Wang, Z. Lin, and M. Guo, "Self-alignment MEMS IMU method based on the rotation modulation technique on a swing base," *Sensors*, vol. 18, no. 4, p. 1178, 2018.
[19] S. Du, "Rotary inertial navigation system with a low-cost MEMS IMU and its integration with GNSS," Ph.D. dissertation, Calgary Univ., Calgary, AB, Canada, 2015.
[20] S. Zheng, H. Dong, R. Zhang, Z. Huang, and J. Wang, "Angle estimation of a single-axis rotation: A practical inertial-measurement-unit-based method," *IET Sci. Meas. Technol.*, vol. 11, no. 7, pp. 892–899, 2017.
[21] Z. Zhou, Z. Tan, X. Wang, and Z. Wang, "Modified dynamic north-finding scheme with a fiber optic gyroscope," *IEEE Photon. J.*, vol. 10, no. 2, Apr. 2018, Art. no. 6801510.
[22] Z. Yuan and W. Ting, "A method of coarse alignment for FOG based inertial platform system using rotation modulation," in *Proc. Chin. Control Decis. Conf. (CCDC)*, Shenyang, China, Jun. 2018, pp. 4356–4360.
[23] Z. Deng, M. Sun, B. Wang, and M. Fu, "Analysis and calibration of the nonorthogonal angle in dual-axis rotational INS," *IEEE Trans. Ind. Electron.*, vol. 64, no. 6, pp. 4762–4771, Jun. 2017.
[24] W. Gao, Y. Zhang, and J. Wang, "Research on initial alignment and self-calibration of rotary strapdown inertial navigation systems," *Sensors*, vol. 15, no. 2, pp. 3154–3171, 2015.
[25] J. Collin, M. Kirkko-Jaakkola, and J. Takala, "Effect of carouseling on angular rate sensor error processes," *IEEE Trans. Instrum. Meas.*, vol. 64, no. 1, pp. 230–240, Jan. 2015.
[26] S. Stancin and S. Tomažic, "Angle estimation of simultaneous orthogonal rotations from 3D gyroscope measurements," *Sensors*, vol. 11, no. 9, pp. 8536–8549, 2011.
[27] S. Tomažič and S. Stančin, "Simultaneous orthogonal rotation angle," *Electro. Technol. Rev.*, vol. 78, pp. 7–11, 2011.
[28] Q. Liang, Y. A. Litvinenko, and O. A. Stepanov, "Method of processing the measurements from two units of micromechanical gyroscopes for solving the orientation problem," *Gyroscopy Navigat.*, vol. 9, no. 4, pp. 233–242, 2018.
[29] B. Johnson, K. Christ, D. Endean, B. Mohr, R. Supino, H. French, and E. Cabuz, "Tuning fork MEMS gyroscope for precision northfinding," in *Proc. DGON Inertial Sensors Syst. Symp. (ISS)*, Karlsruhe, Germany, Sep. 2015, pp. 19–27.
[30] J. Lu, X. Liu, and R. Zhang, "Calibration, alignment, and dynamic tilt maintenance method based on vehicular hybrid measurement unit," *IEEE Sensors J.*, vol. 19, no. 17, pp. 7243–7253, Sep. 2019.
[31] F. O. Silva, E. M. Hemerly, and W. C. L. Filho, "Influence of latitude in coarse self-alignment of strapdown inertial navigation systems," in *Proc. IEEE/ION Position Location Navigat. Symp.—PLANS*, May 2014, pp. 1219–1226.
[32] D. Jurman, M. Jankovec, R. Kamnik, and M. Topič, "Calibration and data fusion solution for the miniature attitude and heading reference system," *Sens. Actuators A, Phys.*, vol. 138, no. 2, pp. 411–420, 2007.
[33] Analog Devices. (2019). *Official Website Compact, Precision Six Degrees of Freedom Inertial Sensor ADIS16445, Datasheet*. [Online]. Available: https://www.analog.com/en/products/adis16445.html
[34] Y. Wu, D. Zou, P. Liu, and W. Yu, "Dynamic magnetometer calibration and alignment to inertial sensors by Kalman filtering," *IEEE Trans. Control Syst. Technol.*, vol. 26, no. 2, pp. 716–723, Mar. 2018.
[35] Y. Zhang, B. Zhou, M. Song, B. Hou, H. Xing, and R. Zhang, "A novel MEMS gyro north finder design based on the rotation modulation technique," *Sensors*, vol. 17, no. 5, pp. 973–995, 2017.

**XIAOWEN CAI** received the M.S. degree in control theory and control engineering from Xiangtan University, in 2008. She is currently pursuing the Ph.D. degree in optical engineering with Beihang University, Beijing, China. Her research interests include related to inertial navigation and integrated navigation.

**CHUNXI ZHANG** received the Ph.D. degree in optical engineering from Zhejiang University, Zhejiang, China, in 1996. He is currently a Professor with Beihang University, Beijing, China. His research interests include optical fiber sensing technology, inertial navigation, and integrated navigation.

**YANQIANG YANG** received the B.S. degree in measurement-control technology and instrumentation from the North University of China, Taiyuan, China. He is currently pursuing the Ph.D. degree with Beihang University, Beijing, China. His research interests include related to inertial navigation and integrated navigation.

**SHUANG GAO** received the Ph.D. degree in optical engineering from Beihang University, Beijing, China, in 2008. She is currently a Lecturer in optical engineering with Beihang University. Her research interests include inertial navigation and inclinometer for petroleum exploration wells.

**RUOYU ZHANG** received the B.S. degree in automation from the China University of Petroleum. She is currently pursuing the M.S. degree in optical engineering with the Beijing University of Aeronautics and Astronautics. Her research interests include calibration technology and inertial navigation.